Available online at www.sciencedirect.com

ScienceDirect

Proceedings of the Combustion Institute 37 (2019) 4389–4397

Proceedings of the Combustion Institute

www.elsevier.com/locate/proci

In-situ gasification chemical looping combustion of plastic waste in a semi-continuously operated fluidized bed reactor

Jinchen Ma [a], Jinxing Wang [a,b], Xin Tian [a], Haibo Zhao [a,*]

[a] *State Key Laboratory of Coal Combustion, Huazhong University of Science and Technology, Wuhan 430074, PR China*
[b] *Department of Thermal Engineering, Tsinghua University, Beijing 100084, PR China*

Received 1 December 2017; accepted 6 July 2018
Available online 29 July 2018

Abstract

Conventional air incineration of plastic waste has been considered as one of important sources of polychlorinated dibenzo-p-dioxins and dibenzofurans (PCDD/Fs) through *de novo* synthesis and precursor conversion. Chemical looping combustion (CLC) is an attractive technology for the conversion of plastic wastes to energy with the potential to drastically suppress the formation of PCDD/Fs. In this paper, the *i*G-CLC (*in-situ* gasification CLC) experiments of plastic waste were implemented in a semi-continuously operated fluidized bed reactor, which actually simulates the fuel reactor of a continuously-operated interconnected fluidized bed reactor. A kind of low-cost material, natural iron ore without/with 5 wt% CaO adsorbent through the ultrasonic impregnation method, was used as oxygen carrier (OC). Firstly, some key performances of the reactor system, such as the relevance of the bed inventory to the flow rate of fluidizing agent as well as the relationship between the feeding rate and overflow rate of OC, were calibrated. Then, 90 min of single experiment was conducted for each experimental case and an accumulative operation of more than 10 h was attained. Typically, the combustion efficiency can reach at about 98%, and both the carbon conversion and CO_2 yield can approach to 95% at 900 °C and input thermal power of 150 W with a mixture of 5 vol% H_2O and 95 vol% N_2 as the fluidizing agent ($U_{FR}/U_{mf} = 3$). Moreover, the results obtained in the semi-continuously operated fluidized bed reactor demonstrated that CaO decoration to iron ore is conductive to suppressing the formation of chlorobenzene (as a toxic matter and precursor/intermediate of PCDD/Fs) and does not obviously deteriorate the OC performance.

Keywords: Semi-continuously operated fluidized bed reactor; In-situ gasification chemical looping combustion; Plastic waste; CaO-decorated iron ore; Chlorobenzene

1. Introduction

Plastic, as a typical municipal solid waste (MSW), is a potentially valuable fuel due to its high calorific value and embodied energy. While

* Corresponding author.
E-mail address: hzhao@mail.hust.edu.cn (H. Zhao).

https://doi.org/10.1016/j.proci.2018.07.032

serious environmental pollution may occur due to the emission of toxic by-products including polychlorinated dibenzo-p-dioxins (PCDDs) and dibenzofurans (PCDFs) during conventional air incineration processes of chlorine contained plastic waste (PW) [1,2]. Factually, the gaseous O_2 presented in the conventional waste incinerator not only participates in carbon gasification and rearrangement as an oxygen source during the *de novo* synthesis process of PCDD/Fs [3], but also promotes the chlorination process by generating Cl_2 (more reactive) via Deacon reaction (R1: $4HCl + O_2 \rightarrow 2Cl_2 + 2H_2O$) [4,5]. Since the formation of PCDD/Fs (via either the *de novo* synthesis route or the precursor conversion (high-temperature homogeneous reactions or low-temperature catalytic-assisted heterogeneous reactions) route) is always involved in the chlorination of the benzene [3], an O_2-free atmosphere (consequently a Cl_2-deficient atmosphere) will be advantageous to *in-situ* inhibition of PCDD/Fs during the thermal treatment processes of PWs. Chemical looping combustion (CLC), which utilizes lattice oxygen rather than gaseous oxygen source for fuel combustion in fuel reactor, so as to create an O_2-free combustion atmosphere, has emerged as a promising technology for waste management [6–8].

CLC has been widely investigated at different scales [9–11], mainly focusing on inherent CO_2 separation. The CLC system is composed of two interconnected but atmosphere-isolated fluidized bed reactors, denoted as air reactor (AR) and fuel reactor (FR). Oxygen carrier (OC) circulates continuously to transport active oxygen from the air (in AR) to the fuel (in FR). In this way, direct reaction between fuel and air can be avoided, which is also the starting point of utilizing CLC to dispose of chlorine contained wastes (e.g., plastic waste, sewage sludge, kitchen waste and waste paper residue). To this end, the new waste management technology is capable of attaining high-efficient energy recovery of wastes, PCDD/Fs inhibition and CO_2 capture simultaneously.

Applicable OC is critical for the industrial implementation of the CLC technique [12,13]. As a common material, iron-based OC has been considered as a promising OC in *in-situ* gasification CLC (*i*G-CLC) of plastic waste [14–17]. To be more specific, iron ore was highlighted as a very attractive OC material because of its abundant reserve, low price, good fluidization ability and acceptable reactivity [13]. Further, *in-situ* dechlorination during the *i*G-CLC processes via decorating chlorine adsorbent on OC particles has been considered as one of the significant ways to lower available chlorine source and therefore inhibits the PCDD/Fs formation [14–17]. In our previous works, the feasibility of dechlorination using different adsorbents (CaO, K_2O, Na_2O) had been investigated when using HCl-containing syngas as fuel and synthetic 60 wt% Fe_2O_3/40 wt% Al_2O_3 as OC, and CaO was selected as the optimal adsorbent [14]. Relevant experimental parameters were also determined in a batch fluidized-bed reactor with plastic wastes as the fuel [15]. Following that, the performances of nature iron ore as OC for the CLC tests of HCl-containing syngas and plastic waste were further evaluated [17]. Eventually, the ultrasonic impregnation method was considered as the suitable CaO decoration method for the natural iron ore and 5 wt% was selected as the applicable loading content.

Up to now, *i*G-CLC of plastic waste was only demonstrated in the batch-operated fluidized-bed reactor, in which the fluidizing agent was periodically switched between air and CO_2/H_2O to simulate the AR and FR respectively, and OC particles was always loaded in the same fluidized bed reactor. Actually, for the industrial application of *i*G-CLC of plastic waste, it is more practical to adopt the operation mode of the interconnected fluidized-bed reactor, which can be retrofitted from the conventional circulating fluidized bed [18]. In the interconnected fluidized bed, OC particles circulate between two reactors to transport the active lattice oxygen as well as heat, and fuel is always fed into the FR. Certainly, the continuous operation of *i*G-CLC in the interconnected fluidized bed reactor is crucially important to test the long-term performance of OC particles and optimize the reactor configuration and operational window. However, it is not an easy task to design an interconnected fluidized-bed reactor for plastic wastes, let alone to construct or operate it. As an intermediate step from the batch-operated fluidized-bed reactor to the continuously-operated interconnected fluidized-bed reactor, we designed and assembled a semi-continuously operated fluidized-bed reactor in this work, which only simulated the fuel reactor of a real *i*G-CLC system, to test the physiochemical behavior of OCs, the combustion performance, the emission of organic compounds and the feasibility of the new waste management technology during a relatively long-term *i*G-CLC process.

In this work, the reactor was first calibrated to measure the bed inventory as a function of superficial fluidization velocity, and to determine the relation between the OC feeding and overflow rate. The appropriate experimental parameters for stable operation of the facility were attained. The effects of superficial fluidization velocity and solid circulation rate on the carbon conversion, CO_2 yield and combustion efficiency were then analyzed. Furthermore, a representative experimental case was selected to examine the effects of CaO decoration to raw iron ore on the emission of chlorobenzene (as a toxic matter and precursor/intermediate of PCDD/Fs) and the OC characteristics. The organic compounds, including chlorobenzene, of exhaust gases were absorbed by toluene solutions and subsequently measured semi-quantitatively using a

Table 1
Proximate and ultimate analyses of the perfusion tube.

Proximate analysis (wt%, as received)				Ultimate analysis (wt%, d.a.f.)						Lower heating value (MJ/kg, db)
Moisture	Volatiles	Ash	FC	C	H	N	S	O	Cl	
0.03	93.79	6.10	0.08	73.89	10.82	0.72	0.16	3.39	4.92	33.87

gas chromatograph–mass spectrometer (GC–MS). In addition, the crystalline phases of these fresh and used OC particles were determined by an X-ray diffraction (XRD), and the morphologies and surface compositions were characterized by an Environmental Scanning Electron Microscope coupled with an Energy Dispersive X-Ray spectroscopy system (ESEM–EDX).

2. Experimental

2.1. Materials

Perfusion tube, as a representative chlorine contained plastic waste, was studied in this work. The proximate and ultimate analyses of the perfusion tube are listed in Table 1. Its ash components are presented in Table S1, supplementary materials (SM). A kind of natural iron ore (Fe_2O_3, 81.89 wt%) was used as OC in the *i*G-CLC of plastic waste. The ultrasonic impregnation method was adopted as the decoration method for adding foreign ions (Ca^{2+}) into the fresh iron ore. The detailed descriptions of the physical and chemical properties of fresh iron ore and preparation method of CaO-decoration iron ore can be found in Section S1 of SM.

2.2. Apparatus and procedure

The semi-continuously operated fluidized-bed reactor is schematically shown in Fig. 1. The system consists of a gas supplying unit, a fresh OC feeding unit, a plastic waste feeding unit, a fluidized-bed reaction unit, an OC collector, a filter, toluene solution, an electric condenser and an on-line gas analyzer (Gasboard-3151). A straight stainless steel tube (inner diameter, ID = 54 mm; height, H = 1280 mm) with a porous distributor located at 715 mm from the bottom is used as the reaction chamber (ID = 54 mm and H = 585 mm, as shown in Fig. 1.), and the entrance of plastic waste and the exit of OC particles are located at 50 mm and 105 mm from the distributor, respectively. In order to ensure the separation of OC from the exhaust gas, the reaction chamber is connected with an expanding straight stainless steel tube (ID = 180 mm, H = 500 mm). The straight stainless steel tube is electrically heated by two furnaces for the reaction zone and the fluidizing gas. The thermocouples and pressure sensors are installed around the feed port of plastic waste (T1 as the temperature of reaction zone, P1), the hopper bottom (T2, P2) and the preheating region to monitor the furnace temperatures. The temperature and pressure values in the reactor were simultaneously recorded by a data logger connected to the computer.

The exhaust gas was first led to a filter to capture particulate matters (ash) and then went through the toluene solution for absorbing the organic compounds under the ice-bath condition. The organic matters captured by the toluene solution were measured by the GC–MS (7890A/5975C, Agilent) with Agilent 19091S column. Next, the off gas was led into an electric cooler to remove the steam carried by gas, and then to the on-line gas analyzer to measure the concentrations of CO_2, CO, CH_4, H_2 and O_2. One special characteristic of the semi-continuously operated fluidized bed reactor is that the OC and plastic waste are continuously introduced into the reactor through two screw feeders, respectively. The rotation speeds of the two screw feeders can be accurately controlled to determine the feeding rate of plastic waste (corresponding to the thermal power) and the feeding rate of fresh OC (namely solid circulation rate).

In this work, 900 °C was selected as the experimental temperature, which had been optimized in our previous publication [15]. The mixture of 5 vol% H_2O and 95 vol% N_2 was specified as the fluidizing agent. H_2O is used as the gasification agent and N_2 is used as the balance gas for the data processing based on the N_2 balance. The feeding rate of plastic waste at 0.265 g/min was determined to meet the 150 W input thermal power (which is equal to the feeding rate multiplying by the low heating value of the plastic waste. The typical *i*G-CLC experiment of plastic waste is as follows: the fresh OC particles at oxidation state were first introduced into the reactor through the hopper as bed material, and then the reactor was heated in the reduction atmosphere to 900 °C. Then, fresh OC particles (fully oxidized previously) were loaded into the hopper through the OC screw feeder and the precise mass rates were controlled by the specified rotation speeds. Meanwhile, the used OC particles would flow out of the reactor and be stored into the sealed storage tank. Once a stable operation was achieved, PW particles were introduced the reactor through the PW feeder.

A detailed reactor description and experimental procedures can be found in Section S2, SM.

In the *i*G-CLC tests of plastic wastes, the OC feeding rate was determined according to the

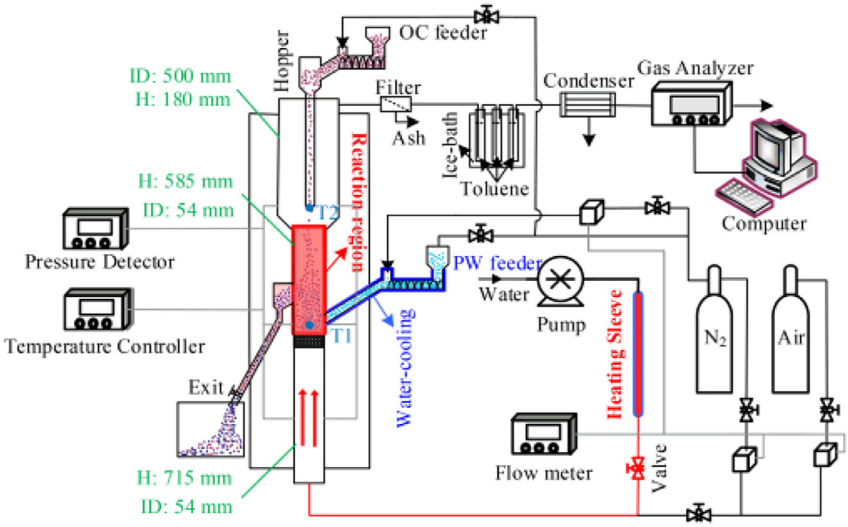

Fig. 1. Overview of the semi-continuously operated fluidized-bed reactor.

supply oxygen ratio (λ):

$$\dot{m}_{OC} = \lambda \times \dot{n}_{O,PW} \times 6M_{Fe_2O_3}/\beta_{Fe_2O_3} \quad (1)$$

$$\dot{n}_{O,PW} = \dot{m}_{PW}\left(\frac{2\beta_C}{M_C} + \frac{2\beta_S}{M_S} + \frac{\beta_H}{2M_H} - \frac{\beta_O}{M_O} - \frac{\beta_{Cl}}{2M_{Cl}}\right) \quad (2)$$

where β_i is the mass fraction of active component i (Fe_2O_3) in the OCs or (N, C, S, H, O, Cl) in the plastic waste, and M_i is the molar mass of species i. $\dot{m}_{PW}$ and $\dot{n}_{O,PW}$ are the mass rate of plastic waste fed into the reactor and the oxygen demand molar rate of plastic waste, respectively. Equation (2) was based on the assumption that plastic wastes are only oxidized to N_2, CO_2, SO_2 and H_2O, and HCl is the only form of chlorine-containing reactants. The supply oxygen ratio is 2.5 here, which is determined as the optimal λ in our previous investigations [15].

2.3. Data evaluation

During the *i*G-CLC of plastic waste, the molar flow of inlet N_2 (F_{N_2}) under the standard conditions is known, and the molar flow of gaseous product species i, $F_{i,out}$ ($i = CH_4$, H_2, CO and CO_2) can be calculated by N_2 balance as:

$$F_{i,out} = F_{N_2}\chi_i \Big/ \left(1 - \sum_i \chi_i\right) \quad (3)$$

where χ_i is the molar fraction of gaseous product species i ($i = CH_4$, H_2, CO and CO_2) in the exhaust gas.

The carbon conversion, γ_C, was calculated as:

$$\gamma_C = 12\left(F_{CO,out} + F_{CH_4,out} + F_{CO_2,out}\right) \Big/ \left(\dot{m}_{PW}\beta_C\right) \quad (4)$$

The CO_2 yield (η_{CO_2}), which denotes the ratio of CO_2 concentration to the total carbonaceous gases concentration in the flue gas, was defined as

$$\eta_{CO_2} = \chi_{CO_2}/(\chi_{CO} + \chi_{CH_4} + \chi_{CO_2}) \quad (5)$$

The combustion efficiency of plastic waste, $\varphi_{comb,FR}$, was calculated by integrating the molar flow of gaseous product species i in the flue gas with the oxygen demand of plastic waste:

$$\varphi_{comb,FR} = \left[1 - \left(F_{CO,out} + 4F_{CH_4,out} + F_{H_2,out}\right)/\dot{n}_{O,PW}\right] \times 100\% \quad (6)$$

For these experimental cases, the average carbon conversion ($\gamma_{ave,C}$), average CO_2 yield (η_{ave,CO_2}) and average combustion efficiency ($\varphi_{ave,comb,FR}$) within 90 min continuous operation were calculated as:

$$\gamma_{ave,C} = \int_0^\tau \gamma_C dt \Big/ \tau;\ \eta_{ave,CO_2} = \int_0^\tau \eta_{CO_2} dt \Big/ \tau;$$

$$\varphi_{ave,comb,FR} = \int_0^\tau \varphi_{comb,FR} dt \Big/ \tau \quad (7)$$

where τ is the continuous operation time.

3. Result and discussion

3.1. The performance test of semi-continuously operated fluidized bed reactor

In the semi-continuously operated fluidized-bed reactor, the bed inventory depends on the flow

Table 2
The feed rate and overflow rate of OC under typical conditions.

U_{FR}/U_{mf}	Flow rate (L/min)	Bed inventory (g)	Total OC feeding (g)	Total OC overflowing (g)	Difference (g/min)
3	2.69	425	478.2	482.6	0.44
4	3.58	364	478.2	472.5	−0.57
5	4.48	301	478.2	486.3	1.81
4	3.58	364	637.6	649.2	1.16

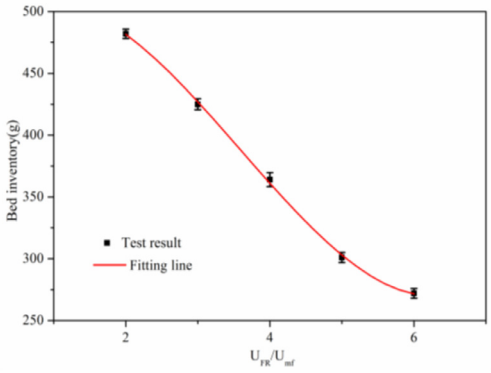

Fig. 2. The corresponding relation between U_{FR}/U_{mf} and bed inventory (error bar was from 3 repeated tests).

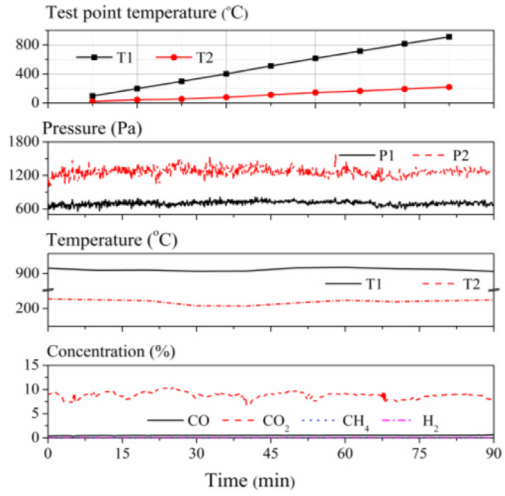

Fig. 3. Temperatures, pressures and gas concentrations during a 90 min operation.

rate of fluidizing agent (presented as U_{FR}/U_{mf} here, where U_{FR} is the fluidizing agent velocity in the FR, and U_{mf} is the minimum fluidization velocity). As shown in Fig. 2, a higher U_{FR}/U_{mf} would eventually lead to a smaller bed inventory. Additionally, it was found that the bed inventory has little relation with the mass rate of OC. Table 2 summarizes the differences between the total feeding and overflowing amounts of OC in 10 min under typical conditions. The absolute difference is always less than 1.81 g/min. When $U_{FR}/U_{mf} = 4$, the bed inventory in reactor basically maintains at 364 g with the variation of OC feeding rate (ranged in 47.82–63.76 g/min). It means that there existed a balance between the feeding rate and overflow rate of OC when reaching the stable and continuous operation. Actually, the OC overflow rate can be automatically adjusted to balance the OC feeding rate.

In order to further evaluate the stability and operability of the semi-continuously operated fluidized-bed system, a representative experimental case of 90 min (OC bed inventory of 364 g, the mixture of 5 vol% H_2O and 95 vol% N_2 was used as the fluidizing agent, input thermal power of 150 W and OC feeding rate of 47.82 g/min) was conducted to detect the temperatures and gage pressures of two test points as well as gas concentrations during the continuous operation. Figure 3(a) exhibits the accurate temperature rising processes of the reaction zone (T1, 50 mm above the distributor) and the expanding section (T2, around the hopper bottom). Figure 3(b) and (c) shows that the pressures and temperatures during the long-term operation process were basically stable. The gas concentrations shown in Fig. 3(d) fluctuated slightly, which should be attributed to the irregular breakage of bubbles. In summary, the semi-continuously operated fluidized-bed system could satisfy the experimental condition needed in this work.

3.2. The effects of key operation parameters

The effects of volume flow rate of fluidizing agent (U_{FR}/U_{mf}) and mass rate of OC on the average carbon conversion, CO_2 yield and combustion efficiency were investigated at 900 °C within a 90 min continuous operation for each case. As shown in Fig. 4, the higher the superficial fluidization velocity is, the smaller the average carbon conversion, CO_2 yield and average combustion efficiency will be. Higher superficial fluidization velocity would shorten the residence time of plastic waste and OC in reaction zone, which degrades the gas–solid contact leading to incomplete PW conversion. Moreover, higher superficial fluidization velocity means less bed inventory (as shown in Fig. 2), thus less active oxygen was provided [15]. All these explained well the inferior *i*G-CLC performances at a higher superficial fluidization velocity.

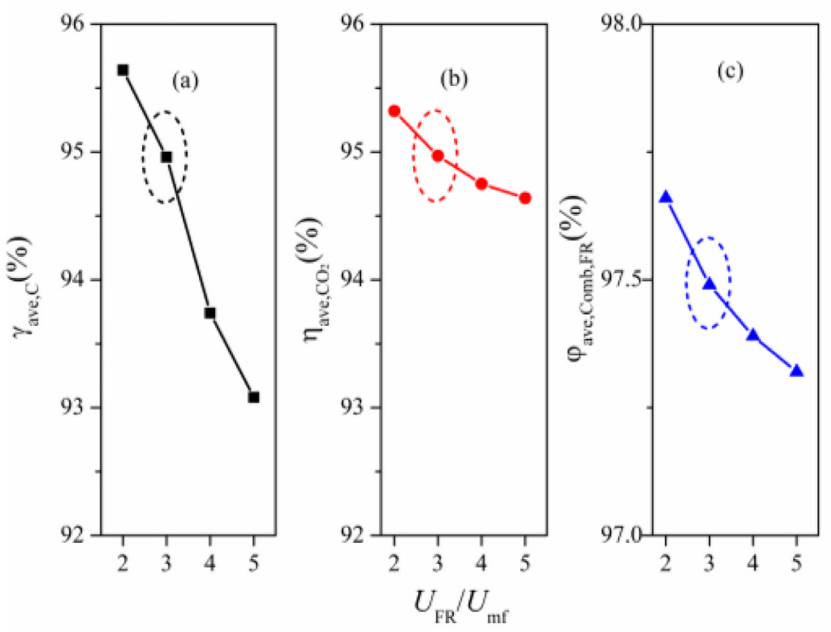

Fig. 4. The evaluation indexes under different U_{FR}/U_{mf}: (a) average carbon conversion (b) average CO_2 yield (c) average combustion efficiency.

Table 3
The evaluation indexes for two kinds of OC particles.

OC	$\gamma_{ave,C}$ (%)	η_{ave,CO_2} (%)	$\varphi_{ave,comb,FR}$ (%)
Raw iron ore	96.36	95.33	97.82
CaO-decorated iron ore	94.96	94.97	97.49

Figure 5 exhibits the variations of the average carbon conversion, average CO_2 yield as well as average combustion efficiency as a function of mass rate of OC. All of these parameters showed an upward trend with the increase of mass rate of OC due to the enhancement of lattice oxygen by higher mass rate of OC, which is conducive to the pyrolysis and conversion of PW [15]. It should be noted that the improvement degree of these *i*G-CLC performance indexes (either for the average CO_2 yield or the average combustion efficiency) from 31.88 g/min to 47.82 g/min of OC mass rate is markedly greater than that from 47.82 g/min to 63.76 g/min. In this sense, 47.82 g/min should be the applicable mass rate of OC when the input thermal power is 150 W (corresponding to the PW feeding rate of 0.265 g/min).

3.3. Comparison with raw iron ore

In this section, the effect of CaO decoration to iron ore on the *i*G-CLC performance of plastic waste was studied at the representative experimental case mentioned above. Table 3 presents a comparison of the *i*G-CLC indexes for the two kinds of OCs. The average carbon conversion, average CO_2 yield and average combustion efficiency with CaO-decorated iron ore as OC were slightly lower than those of raw iron ore. These deficiencies can be properly addressed by enhancing the OC circulation rate as discussed in Section 3.2.

The organic compounds were measured by a GC–MS to semi-quantitatively clarify the effect of CaO decoration on the emission of chlorobenzene in *i*G-CLC process. Figure 6 shows the total ion chromatography of toluene solutions for two *i*G-CLC processes and Table S3 in SM lists these detected organic compounds. It can be found that the abundance values of these main organic compounds (including benzaldehyde, 2,2-dimethyl-Heptane, 2-ethyl-1-Hexanol, decamethyl-cyclopentasiloxane and diethyl undecyloxy-silane) in the two *i*G-CLC processes were at comparable level. Additionally, the abundance value of chlorobenzene using CaO-decoration iron ore as OC was indeed less than that using iron ore as OCs. All these results demonstrated that using CaO-decorated iron ore as OCs to control the emission

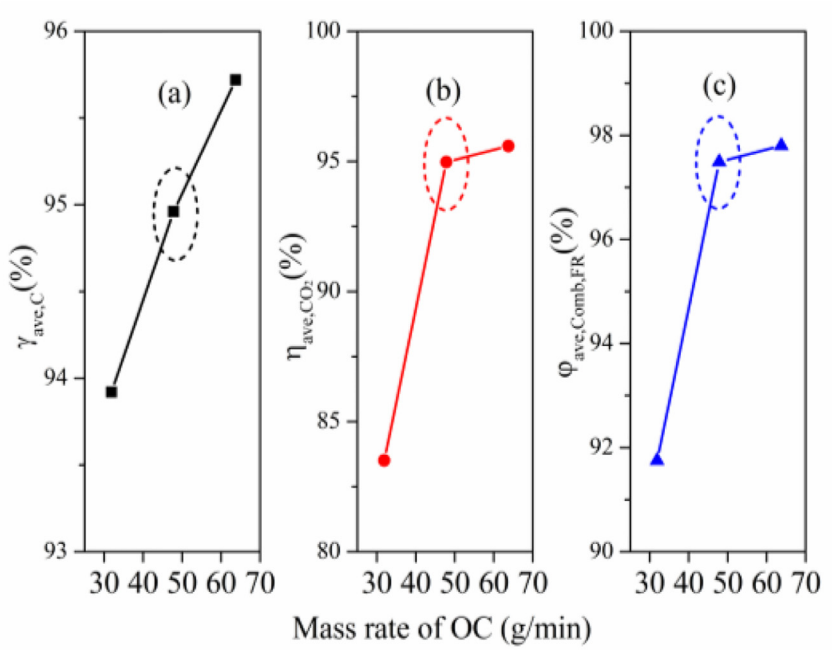

Fig. 5. The evaluation indexes under different mass rate of OC: (a) average carbon conversion (b) average CO_2 yield (c) average combustion efficiency.

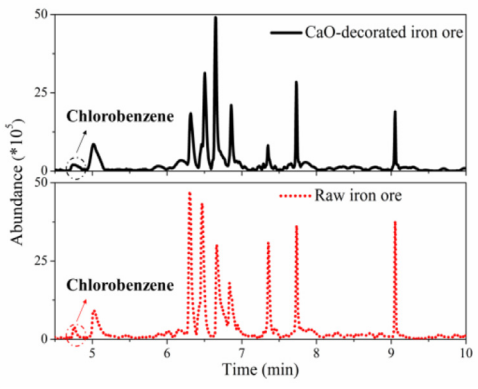

Fig. 6. Total ion chromatography of toluene solutions for two *i*G-CLC processes.

of chlorobenzene during the plastic waste-derived *i*G-CLC process is feasible.

In this work, PCDD/Fs and chlorobenzene cannot be quantified due to the accuracy limitation of the GC–MS. Other higher chlorinated benzenes were not measured. It was worth noting that recently we have quantitatively measured the 17 toxic PCDD/Fs congeners by a high-resolution gas chromatography/high-resolution mass spectrometer (HRGC/HRMS) [16]. Two combustion experiments (conventional air incineration; *i*G-CLC using CaO-decorated Fe_2O_3/Al_2O_3 as oxygen carrier) were conducted in a batch-operated fluidized bed reactor that simulates an *i*G-CLC process. This work verified that the formation of PCDD/Fs can be significantly inhibited via the *i*G-CLC technique. To be more specific, the amount and toxic equivalency quantity of PCDD/Fs can be reduced by an order of magnitude using the *i*G-CLC technique.

3.4. Physicochemical characterization

Figure 7(a) and (c) shows that Fe_2O_3 was the single crystalline phase of iron element in the fresh OC particles, which indicates that both the iron ore and CaO-decorated iron ore OC particles have been adequately oxidized within the preparation process. Notably, Fe_2O_3 was still the main crystalline phase of iron element in used OC particles after 90 min operation, as shown in Fig. 7(b) and (d). It demonstrated that the amount of OC was excessive over plastic waste during the *i*G-CLC experiments. Besides, CaO was presented in the form of $CaOSiO_2$, which should be derived from the ultrasonic impregnation process [17] and subsequent calcination process.

As shown in Fig. 8(a) and (b), C, O, Fe, Al and Si elements were detected on the surface of the fresh and used OC particles, where C is the conducting medium sprayed on the sample for detection. Besides, Ca was observed in Fig. 8(c) and (d), which was derived from CaO decoration. Moreover, when

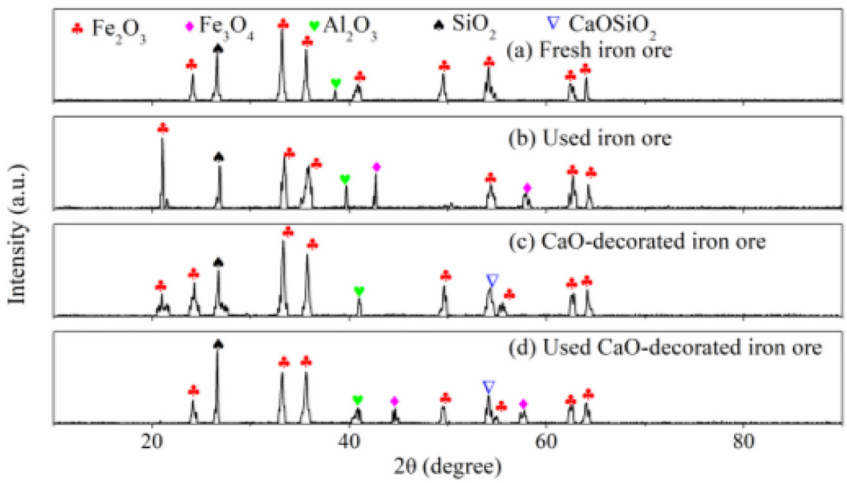

Fig. 7. Phase composition of different kind of iron ores after 90 min operation.

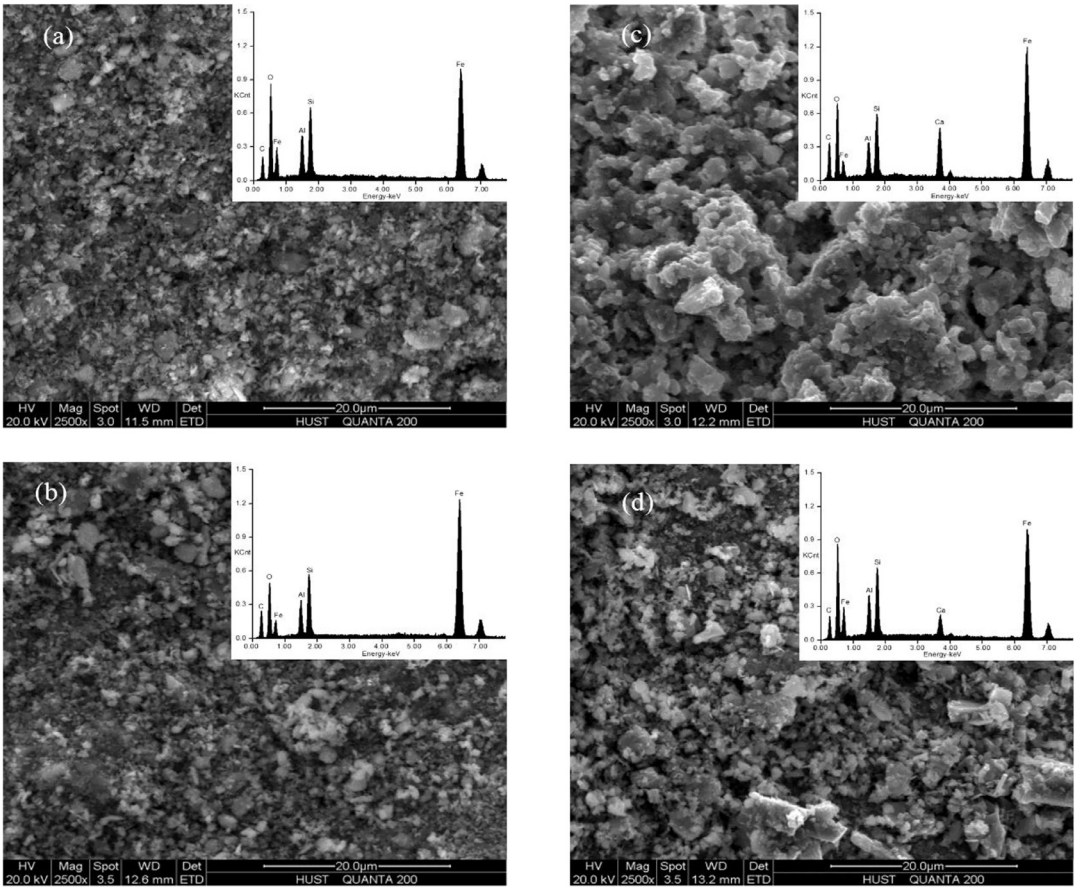

Fig. 8. ESEM images and EDX analyses of the fresh (a) and used (b) iron ore, the fresh (c) and used (d) CaO-decorated iron ore.

comparing to the EDX results of the fresh and used CaO-decorated iron ore OCs, one found that the Ca peak was lowered after being tested in the fluidized bed reactor. This may be caused by CaO loss in the severe fluidizing reaction condition in the reactor. Notably, the used CaO-decorated OC can be reproduced via being washed by a dilute hydrochloric acid solution and then being decorated again [14]. In addition, no obvious sintering/agglomeration problem occurred to the two kinds of used OC particles. As can be concluded, CaO decoration to the iron ore does not clearly incur the adverse effect on OC particles.

4. Conclusions

CLC provides an O_2-free combustion pattern, which is probably beneficial to inhibit the *de novo* synthesis of PCDD/Fs. Moreover, effective *in-situ* dechlorination during CLC processes may be conducive to suppressing the formation of PCDD/Fs from the conversion of precursors. The *i*G-CLC experiments of plastic waste were conducted in a semi-continuously operated fluidized-bed reactor (which simulates the fuel reactor of a real interconnected fluidized bed reactor in this study) and 5 wt% CaO-decoration iron ore OC was adopted to control the emission of PCDD/Fs. First, the performance of the semi-continuously operated fluidized bed system was tested to demonstrate the stability and operability of the reactor system. Then, both superficial fluidization velocity and solid circulation rate were investigated by analyzing their effects on average carbon conversion, CO_2 yield and combustion efficiency. For a representative experimental case (OC inventory of 364 g, the mixture of 5 vol% H_2O and 95 vol% N_2 was used as the reaction atmosphere, input thermal power of 150 W and OC mass rate of 47.82 g/min), the combustion efficiency was achieved at about 98%, and both the carbon conversion and CO_2 yield were approximatively 95%. The effects of CaO decoration to iron ore on the *i*G-CLC performances and the emission of organic compounds in exhaust gases were also analyzed. These results demonstrated that the CaO-decorated iron ore OC exhibits a slightly lower reactivity than the raw iron ore in plastic waste-derived *i*G-CLC process, however the emission of chlorobenzene can be effectively inhibited. Besides, XRD and ESEM–EDX results indicated that no obvious sintering/agglomeration was observed on the surface of the used OC particles. To sum up, the obtained results in this work can provide useful information for the industrial application of plastic waste-derived *i*G-CLC process with CaO-decorated iron ore as OC.

In this work, we did not measure PCDD/Fs in exhaust gas yet. The accumulative PCDD/Fs and their distribution in continuous *i*G-CLC experiments of plastic waste should be detected to better understand the emission characteristics of PCDD/Fs and the inhibition mechanism of *i*G-CLC technology.

Acknowledgment

These authors were supported by “National Key R&D Program of China (2016YFB0600801)” and “National Natural Science of China (51522603)”.

Supplementary materials

Supplementary material associated with this article can be found, in the online version, at doi:10.1016/j.proci.2018.07.032.

References

[1] H. Tian, J. Gao, L. Lu, D. Zhao, K. Cheng, P. Qiu, *Environ. Sci. Technol.* 46 (2012) 10364–10371.
[2] S.M. Al-Salem, P. Lettieri, J. Baeyens, *Prog. Energy Combust. Sci* 36 (2010) 103–129.
[3] B.R. Stanmore, *Combust. Flame* 136 (2004) 398–427.
[4] N.W. Tame, B.Z. Dlugogorski, E.M. Kennedy, *Prog. Energy Combust. Sci.* 33 (2007) 384–408.
[5] M. Altarawneh, B.Z. Dlugogorski, E.M. Kennedy, J.C. Mackie, *Prog. Energy Combust. Sci.* 41 (2010) 245–274.
[6] X. Niu, L. Shen, H. Gu, S. Jiang, J. Xiao, *Chem. Eng. J.* 268 (2015) 236–244.
[7] P.C. Chiu, Y. Ku, H.C. Wu, Y.L. Kuo, Y.H. Tseng, *Fuel* 135 (2014) 146–152.
[8] Y. Cao, A. Bianca Casenas, W.P. Pan, *Energy Fuels* 20 (2006) 1845–1854.
[9] H. Leion, E. Jerndal, B.M. Steenari, et al., *Fuel* 88 (2009) 1945–1954.
[10] I. Adánez-Rubio, A. Abad, P. Gayán, L.F.D. Diego, F. García-Labiano, J. Adánez, *Fuel Process. Technol.* 124 (2014) 104–114.
[11] J. Ma, H. Zhao, X. Tian, et al., *Appl. Energy* 157 (2015) 304–313.
[12] J. Adanez, A. Abad, F. García-Labiano, P. Gayan, L.F.D. Diego, *Prog. Energy Combust. Sci.* 38 (2012) 215–282.
[13] M. Matzen, J. Pinkerton, X. Wang, Y. Demirel, *Int. J. Greenhouse Gas Control* 65 (2017) 1–14.
[14] J. Wang, H. Zhao, *Combust. Flame* 162 (2015) 3503–3515.
[15] J. Wang, H. Zhao, *Fuel* 165 (2016) 235–243.
[16] H. Zhao, J. Wang, *Combust. Flame* 191 (2018) 9–18.
[17] J. Wang, H. Zhao, *Energy Fuels* 30 (2016) 5999–6008.
[18] S.K. Haider, G. Azimi, L. Duan, et al., *Appl. Energy* 163 (2016) 41–50.